VOLUME 10 ISSUE 2 2024

ISSN 2454 – 3055

INTERNATIONAL JOURNAL OF ZOOLOGICAL INVESTIGATIONS

Forum for Biological and Environmental Sciences

Published by Saran Publications, India

International Journal of Zoological Investigations Vol. 10, No. 2, 1341-1352 (2024)

International Journal of Zoological Investigations
Contents available at Journals Home Page: www.ijzi.net
Editor-in-Chief: Prof. Ajai Kumar Srivastav
Published by: Saran Publications, Gorakhpur, India

ISSN: 2454-3055

Comparative Analysis of Various Extraction Methods upon the Yield and Chemical Composition of Bacterial Cellulose Produced by *Novacetimonas hansenii* OR418572

Joseph Anju and Sepperumal Umamaheswari *

Department of Zoology, Thanthai Periyar Government Arts and Science College (Affiliated to Bharathidasan University), Tiruchirapalli, Tamil Nadu, India

**Corresponding Author*

Received: 6th June, 2024; **Accepted:** 27th August, 2024; **Published online:** 30th December, 2024

https://doi.org/10.33745/ijzi.2024.v10i02.137

Abstract: Bacterial cellulose (BC) is a promising biopolymer produced by aerobic bacteria. Compared with plants, BC has many superior qualities, like high water-holding capacity, biocompatibility, high purity, crystallinity, and biodegradability. Its unique physio-chemical and morphological features are helpful in various industries like paper making, food packaging, and pharmaceutical. The purification process plays a significant role in determining the quality of BC. BC produced in the air-liquid interface of the fermentation medium is subjected to alkali treatment for purification. The proper setup and subsequent characterization are essential for experiments on biomaterials. BC is used for various medical applications, including medicine. This study aims to determine the influence of various purification processes on BC and introduce the best purification method. Method of purification is not affecting the weight of BC. Chemical changes are reflected in FTIR studies, and the morphological changes are visible on SEM images. Even though there are not significant chemical changes, the morphological changes are observed.

Keywords: Bacterial cellulose, Biopolymer, Fourier transform infrared, Scanning Electron Microscopy, Purification

Citation: Joseph Anju and Sepperumal Umamaheswari: Comparative analysis of various extraction methods upon the yield and chemical composition of bacterial cellulose produced by *Novacetimonas hansenii* OR418572. Intern. J. Zool. Invest. 10(2): 1341-1352, 2024.

https://doi.org/10.33745/ijzi.2024.v10i02.137

Introduction

Bacterial cellulose is a promising product in this modern world. The main reason is it's wide variety of applications in various fields such as scaffolds for tissue engineering applications, optically transparent composites, artificial skin for severe burn patients, wound healing applications, skin tissue repair, artificial blood vessels for microsurgery, sound transducing membranes, high-quality paper manufacturing and thickening and stabilising agents in the food industry (Tsouko *et al.*, 2015). Because of its unique properties like high water holding capacity, high degree of

polymerisation, mechanical strength, purity, high crystallinity (Saibuatong and Phisalaphong, 2010; Moniri *et al.*, 2017), nanostructure (Chen *et al.*, 2010), transparency, biocompatibility and biodegradability (Guzel and Akpinar, 2019) etc. make it more attractive in various fields. There are many bacteria which have the ability to produce bacterial cellulose such as a *Gluconacetobacter*, *Achromobacter*, *Aerobacter*, *Agrobacterium*, *Alcaligenes*, *Azotobacter*, *Rhizobium*, *Sarcina*, *Salmonella*, *Escherichia*, etc. (Huang *et al.*, 2016). Many researchers develop bacterial cellulose from different carbon sources other than glucose. All the factors like different carbon sources, nitrogen sources, different bacterial strain and the purification process affect its structural and functional properties (Kamal *et al.*, 2020). The production process techniques have a significant impact on the amount and quality of cellulose, which is directly reflected in the process economics.

Furthermore, the microbial cellulose produced using these techniques is not entirely pure; it includes certain impurities such as whole *A. xylinum* cells and components of culture broth. Certain purifying techniques lessen the quantity of cells and coloration. Present study focus on the purification techniques and its influences on its structural and functional properties. Purification step is very important because it remove the impurities like cell mass, broth components etc. (Hashim *et al.*, 2021). Appropriate purification method helps to improve the quality of cellulose sheets.

Materials and Methods

Isolation and identification of cellulose producing bacteria:

1 g of decomposed fruit sample was taken and 9 ml of saline was added and serially diluted up to 10^{-9} dilution. 0.1 ml of 10^{-9} dilution was inoculated on standard Hestrin – Schramm agar medium and incubated at 30°C for 48 h and the colony forming units were determined. The selected dominant bacteria were sub cultured in autoclaved nutrient broth for 48 h at 25°C in a rotary shaker. The identification of bacterial strain was done by the employment of 16 S rRNA sequencing.

Cultural conditions of bacterial cellulose:

1 ml of the broth culture of *Novacetimonas hansenii* (OR418572) was inoculated into 100 ml HS medium (2 g glucose, 0.5 g yeast extract, 0.5 g peptone, 0.27 Disodium hydrogen phosphate, 0.115 g citric acid) and incubated at 25°C for a period of nine days.

Purification of bacterial cellulose:

Different kinds of purification strategies were investigated in accordance with variations in treatment time, temperature, and concentration of NaOH. In order to eliminate microorganisms and impurities, the cellulose sheets were subjected to alkali treatment. In method 1, the cellulose sheets were collected washed with distilled water and treated with 2% NaOH at 80°C for 30 min, repeat the same procedure for three times. BC was subsequently washed with distilled water and air-dried overnight to a moisture content of zero before being weighed to determine yield. In method 2, harvested BC sheets washed with distilled water and treated with 4% NaOH at 100°C for 20 min, washed with distilled water until it reaches neutral pH then air-dried overnight. In method 3, instead of 4% NaOH, 0.4% NaOH was used at 80°C for 60 min. In method 4 and 5, harvested BC sheets were subjected to 4% NaOH at 80°C for 60 min and 0.4 % NaOH at 100°C for 20 min, respectively. Washed with distilled water until it reaches neutral pH and air-dried overnight.

Fourier transform infrared (*FT-IR*):

The bacterial cellulose membrane endured FTIR spectroscopy in order to identify the functional groups that are contained within. Utilizing a BIO-RAD spectrometer (Model FTS 40A), Fourier transform infrared (FT-IR) analyses were conducted within the wavenumber of 4000 cm^{-1} to 650 cm^{-1}. The FT-IR spectra were acquired through the accumulation of 32 images with a resolution of 2 cm^{-1}.

Scanning Electron Microscopy (*SEM*):

Utilizing a VEGA3 TESCAN scanning electron microscope (SEM), the surface modifications of bacterial cellulose produced by *Novacetimonas hansenii* (OR418572) were determined. Prior to scanning electron microscopy (SEM), bacterial cellulose sheets were commonly sputter-coated with gold or other metal ions. The analysis was conducted utilizing a large field detector (LFD) and low vacuum 0.68 Torr mode with 10 to 30 kV at magnifications ranging from 6.13 kx to 500 kx.

Results and Discussion

One-way Anova:

Table 1 indicates that there is no significant difference between the weight of cellulose obtained by the purification process 1, 2, 3, 4 and 5. (Method 1: 7.7367±0.76002 mg; Method 2: 7.6967±0.54519 mg; Method 3: 6.5067±0.43924 mg; Method 4: 6.9900 ± 0.84870 mg; Method 5: 7.4700±1.15659 mg). Figure 1 clearly illustrates the changes observed before and after NaOH treatment.

FTIR Analysis:

The FTIR spectrum of cellulose obtained from first purification method is displayed in Figure 2. According to the literature review 3375 cm^{-1} - 3340 cm^{-1} indicates OH stretching vibration (Popescu *et al.*, 2007), the signature band at 2919 cm^{-1} has been attributed to CH stretching vibration. The absorption band at 1559 cm^{-1}, 1281 cm^{-1}, 669 cm^{-1} and 618 cm^{-1} corresponds to CH stretching. 2852 cm^{-1} indicates symmetrical CH_2 stretching vibration of non-cellulose polysaccharides. The absorption peaks around 1651cm^{-1}, 1428 cm^{-1}, and 1372 cm^{-1} indicates C=O stretching, CH_2 bending and CH_3 deformation, respectively. The band at 1337 cm^{-1} has been assigned to OH in plane bending. 1317 cm^{-1} and 1281 cm^{-1} have been ascribed to CH_2 wagging, CH deformation and C-C has been represented by absorption peaks at 1111 cm^{-1} (Table 2). C-O-C functional group has been represented by 1234 cm^{-1}, 1162 cm^{-1}, 1060 cm^{-1} and 895 cm^{-1}. Absorption peaks at 1204 and 1036 have been linked to OH plane bending and C-O stretching vibration.

Figure 3 displays the FTIR spectrum of cellulose acquired by the second purification method. The broad absorption peak at 3480 cm^{-1} has been attributed OH bond stretching. 1760 cm^{-1} and 1653 cm^{-1} have been assigned to C=O bond stretching. 1596 cm^{-1} and 1511 cm^{-1} corresponds to C=C stretching. Absorption peak at 1439 cm^{-1} has been assigned to COOH. 1375 cm^{-1} for CH_3 deformation and 1202 cm^{-1} to OH plane bending. The absorption peaks at 1159 cm^{-1} and 1116 cm^{-1} have been assigned to C-O-C and C-C bond stretching, respectively. Absorption peaks at 865 cm^{-1},685 cm^{-1},665 cm^{-1} and 622 cm^{-1} have been attributed to CH group (Table 3).

The FTIR spectrum of cellulose obtained from third purification process is depicted in Figure 4. OH stretching vibration observed corresponds to 3349 cm^{-1} and 1336 cm^{-1}. The absorption peaks at 2898 cm^{-1}, 1550 cm^{-1} and 618 cm^{-1} have been ascribed to CH bond stretching. The absorption peak at 1647 cm^{-1} corresponds to C=O stretching (Li *et al.*, 2015). The absorption peaks at 1428 cm^{-1}, 1366 cm^{-1}, 1281 cm^{-1} are indicated by CH_2 bending, CH_3 deformation and CH deformation, respectively. The absorption band at 1236 cm^{-1} is linked to C-O-C group. 1161 cm^{-1} for C-O-C bending proves the basic cellulose peaks (Uzyol and Sacan, 2017). 1061 cm^{-1} also attributes to C-O-C. The amorphous band at 897 cm^{-1} has been assigned to C-O-C stretching at β (1-4) glycosidic linkage (Pandey *et al.*, 2014). The absorption peak around 1111 cm^{-1} is another signature band of cellulose which indicates C-C bonds of the monomer units of polysaccharide (Dayal *et al.*, 2013). C-O stretching is shown at 1037 cm^{-1} absorption peak. The peaks around 668 cm^{-1} exhibits CH rocking. OH plane bending has been observed at 1202 cm^{-1} (Table 4).

The cellulose FTIR spectrum obtained by the fourth purification process is shown in Figure 5. The absorption peak at 3348 cm^{-1} has been attributed to hydroxyl group (OH). OH plane

Table 1: One-way analysis of variance showing variation in the quantity of Bacterial cellulose obtained by various purification processes

Methods	Weight of BC (mg) Mean ± SD
1	7.7367 ±0.76002
2	7.6967 ±0.54519
3	6.5067 ±0.43924
4	6.9900 ±0.84870
5	7.4700 ±1.15659
F value	1.320 (NS)
P value	0.327

NS – Not significant; n = 3

Fig. 1: Image of BC before and after purification process.

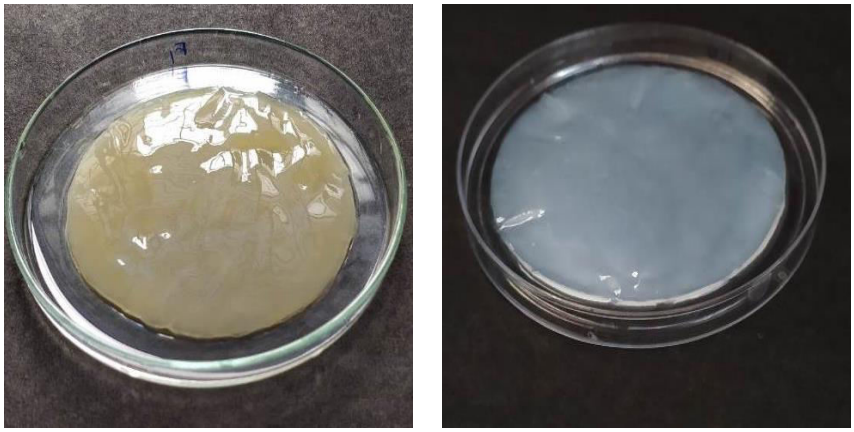

(a) Before (b) After

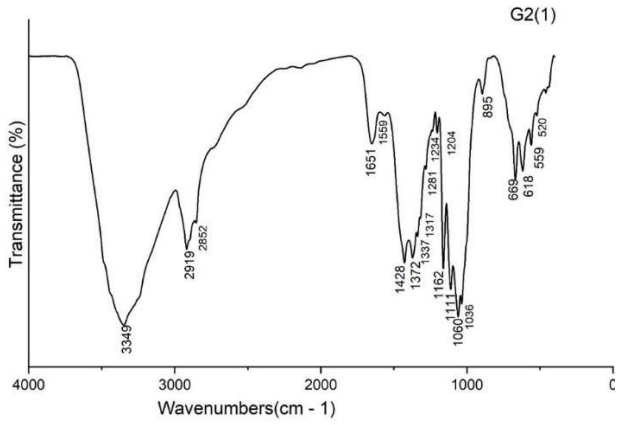

Fig. 2: FTIR spectrum of BC produced by the first purification process.

Table 2: Band assignment of FTIR spectrum of cellulose obtained from first purification method

Wavenumber (cm^{-1})	Functional group	References
3349	OH stretching	Moharram and Mahmoud (2008), Vazquez *et al.* (2013), Hassan *et al.* (2015), Uzyol and Sacan (2017), Hashim *et al.* (2021)
2919	CH stretching	Irham *et al.* (2020), Shezad *et al.* (2010), Amin *et al.* (2012), Sepperumal *et al.*. (2014), Popescu *et al.* (2007), Pandey *et al.* (2014)
2852	Va (CH_2)	Sepperumal *et al.* (2014)
1651	C=O stretching	Li *et al.* (2015)
1559	CH	Irham *et al.* (2020)
1428	CH_2 bending	Hassan *et al.* (2015), Vazquez *et al.* (2013), Pandey *et al.* (2014)
1372	CH_3 deformation	Costa *et al.* (2011)
1337	OH	Castro *et al.* (2012), Costa *et al.*. (2011), Vazquez *et al.* (2013)
1317	CH_2 wagging	Castro *et al.* (2012), Vazquez *et al.* (2013)
1281	CH deformation	Popescu *et al.* (2007)
1234	C-O-C	Umamaheswari and Naveena (2017)
1204	OH plane bending	Popescu *et al.* (2007), Vazquez *et al.* (2013)
1162	C-O-C	Uzyol and Sacan (2017), Casaburi *et al.* (2018), Amin *et al.* (2012), Hassan *et al.* (2015), Auta *et al.* (2017), Pandey *et al.* (2014), Costa *et al.* (2011)
1111	C-C	Dayal *et al.* (2013), Sepperumal *et al.* (2014)
1060	C-O-C	Moosavi and Yousefi (2010), Vazquez *et al.* (2013), Kuo *et al.* (2016)
1036	C-O stretching	Popescu *et al.* (2007)
895	C-O-C	Dayal *et al.* (2013), Pandey *et al.* (2014),
669	CH Rocking	Irham *et al.* (2020)
618	CH	Kondo *et al.* (2016)

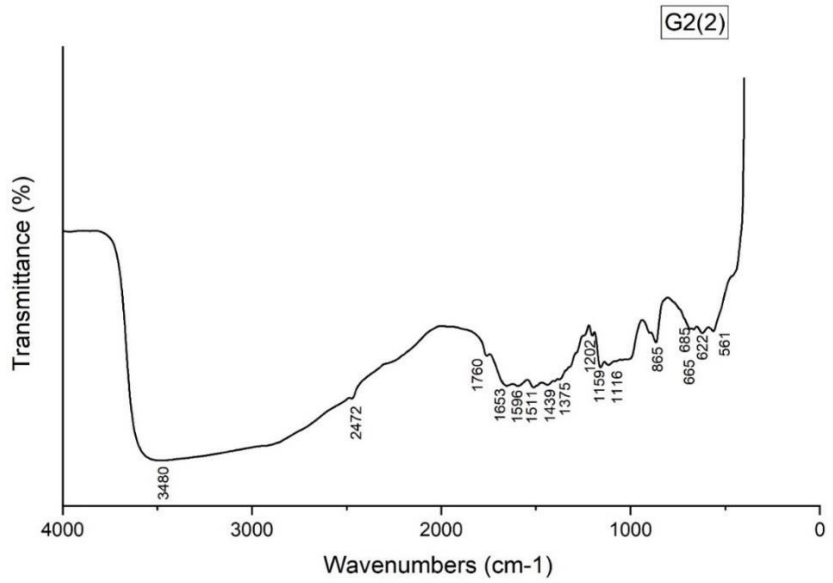

Fig. 3: FTIR spectrum of BC produced by the second purification process.

Table 3: Band assignment of FTIR spectrum of cellulose obtained from second purification method

Wavenumber (cm^{-1})	Functional group	References
3480	OH stretching	Hassan *et al.* (2015), Halib *et al.* (2012)
1760	C=O	Popescu *et al.* (2007)
1653	C=O stretching	Li *et al.* (2015)
1596	C=C stretching	Popescu *et al.* (2007)
1511	C=C	Popescu *et al.* (2007)
1439	COOH	Moosavi and Yousefi (2010), Cakar *et al.* (2014)
1375	CH_3 deformation	Costa *et al.* (2011)
1202	OH, plane bending	Popescu *et al.* (2007), Vazquez *et al.* (2013)
1159	C-O-C	Uzyol and Sacan (2017), Casaburi *et al.* (2018), Amin *et al.* (2012), Hassan *et al.* (2015), Auta *et al.* (2017), Pandey *et al.* (2014), Costa *et al.* (2011)
1116	C-C	Dayal *et al.* (2013), Sepperumal *et al.* (2014)
865	CH out of plane bending	Umamaheswari and Naveena (2017)
685	CH	Kondo *et al.* (2016)
665	CH rocking	Irham *et al.* (2020)
622	CH	Kondo *et al.* (2016)

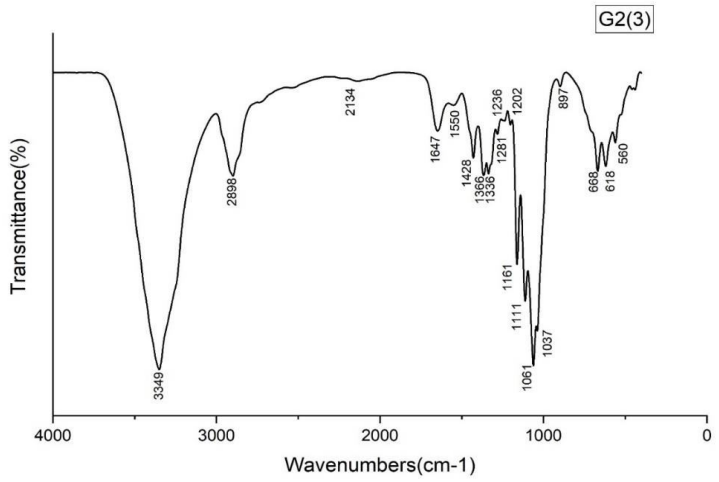

Fig. 4: FTIR spectrum of BC produced by the third purification process.

bending is reflected at 1205 cm^{-1}. The band corresponding to CH stretching is observed at 2921 cm^{-1}. The absorption peak at 1650 cm^{-1} indicates C=O stretching. Absorption band at 1548 cm^{-1} and 618 cm^{-1}, 1427 cm^{-1} and 1400 cm^{-1}, 1375 cm^{-1}, and 668 cm^{-1} indicates CH, CH_2 bending, CH_3 deformation and CH rocking, respectively. The peaks at 1161 cm^{-1}, 1060 cm^{-1} and 892 cm^{-1} assigned to C-O-C. The absorption peak around 1111 cm^{-1} is one of the signature band of cellulose, which indicates C-C bonds of the monomer units of polysaccharide (Dayal *et al.*, 2013). The peak at 1036 cm^{-1} corresponds to C-O stretching (Fig. 5).

The FTIR spectrum of cellulose obtained from fifth purification method is displayed in Figure 6. The most representative bands in the 3700 cm^{-1} – 2700 cm^{-1} region have been assigned to OH inter-molecular and intra-molecular stretching mode. The bands around 2897 cm^{-1} assigned to CH stretching. One of the important peaks of cellulose shown around 1645 cm^{-1} region indicates C=O stretching (Li *et al.*, 2015). The absorption peak around 1111 cm^{-1} is a signature band of cellulose, indicates C-C bonds of the monomer units of polysaccharide (Dayal *et al.*, 2013). 1428 cm^{-1}, 1364 cm^{-1}, 1281 cm^{-1}, 668 cm^{-1} cm^{-1}, 1543 and 619

Table 4: Band assignment of FTIR spectrum of cellulose obtained from third purification method

Wavenumber (cm^{-1})	Functional group	References
3349	OH stretching	(Hashim *et al.*, 2021), (Moharram and Mahmoud, 2008), (Moosavi and Yousefi, 2010), (Hassan *et al.*, 2015), (Uzyol and Sacan, 2017)
2898	CH stretching	(Oliveira *et al.*, 2015)
1647	C=O stretching	(Li *et al.*,2015)
1550	CH	(Irham *et al.*, 2020)
1428	CH_2 bending	(Hassan *et al.*, 2015), (Moosavi and Yousefi, 2010), (Halib *et al.*, 2012), (Pandey *et al.*, 2014)
1366	CH_3 deformation	(Costa *et al.*, 2011)
1336	OH	(Moosavi and Yousefi, 2010), (Castro *et al.*, 2012), (Costa *et al.*, 2011)
1281	CH deformation	(Popescu *et al.*, 2007),
1236	C-O-C	(Sepperumal *et al.*, 2014),
1202	OH plane bending	(Popescu *et al.*, 2007), (Moosavi and Yousefi, 2010)
1161	C-O-C	(Uzyol and Sacan, 2017), (Casaburi *et al.*, 2018), (Amin *et al.*, 2012), (Hassan *et al.*, 2015), (Auta *et al.*, 2017), (Pandey *et al.*, 2014), (Costa *et al.*, 2011)
1111	C-C	(Dayal *et al.*, 2013), (Sepperumal *et al.*, 2014)
1061	C-O-C	(Moosavi and Yousefi, 2010), (Kuo *et al.*, 2016)
1037	C-O stretching	(Popescu *et al.*, 2007)
897	C-O-C	(Dayal *et al.*, 2013), (Pandey *et al.*, 2014)
668	CH Rocking	(Irham *et al.*, 2020)
618	CH	(Kondo *et al.*, 2016)

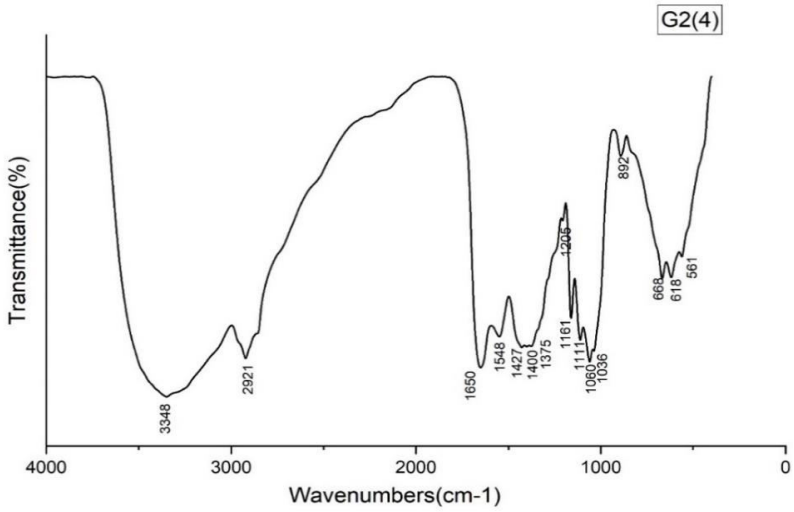

Fig. 5: FTIR spectrum of BC produced by the fourth purification process.

Table 5: Band assignment of FTIR spectrum of cellulose obtained from fourth purification method

Wavenumber (cm $^{-1}$)	Functional group	References
3348	OH stretching	Hashim *et al.* (2021), Moharram and Mahmoud (2008), Vazquez *et al.* (2013), Hassan *et al.* (2015), Uzyol *et al.* (2017)
2921	CH stretching	Irham *et al.* (2020), Shezad *et al.* (2010), Amin *et al.* (2012), Sepperumal *et al.* (2014), Popescu *et al.* (2007), Pandey *et al.* (2014)
1650	C=O stretching	Li *et al.* (2015)
1548	CH	Irham *et al.* (2020),
1427	CH_2 bending	Hassan *et al.* (2015), Vazquez *et al.* (2013), Halib *et al.* (2012), Pandey *et al.* (2014),
1400	CH_2 bending	Kondo *et al.* (2016), Hassan *et al.* (2015)
1375	CH_3 deformation	Costa *et al.* (2011)
1205	OH plane bending	Popescu *et al.* (2007), Vazquez *et al.* (2013)
1161	C-O-C	Uzyol *et al.* (2017),(Casaburi *et al.* (2018), Amin *et al.*, (2012), Hassan *et al.* (2015), Auta *et al.* (2017), Pandey *et al.* (2014), Costa *et al.* (2011)
1111	C-C	Dayal *et al.* (2013), Sepperumal *et al.* (2014)
1060	C-O-C	Moosavi and Yousefi (2010), Vazquez *et al.* (2013), Kuo *et al.* (2016)
1036	C-O stretching	Popescu *et al.* (2007)
892	C-O-C	Dayal *et al.* (2013), Pandey *et al.* (2014)
668	CH Rocking	Irham *et al.* (2020)
618	CH	Kondo *et al.* (2016)

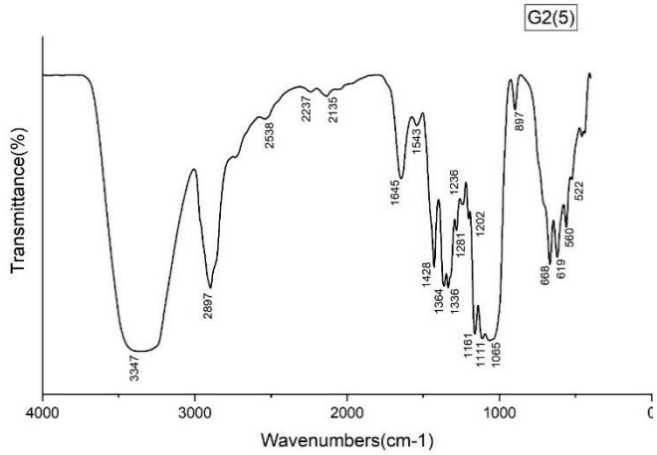

Fig. 6: FTIR spectrum of BC produced by the fifth purification process.

cm^{-1} indicate CH_2 bending, CH_3 deformation, CH deformation, CH rocking and CH group, respectively. 1336 cm^{-1} has been assigned to hydroxyl group and at 1202 cm^{-1} for OH plane bending. Three absorption peaks at 1161 cm^{-1}, 1065 cm^{-1}, and 897 cm^{-1} have been attributed to C-O-C bond stretching (Table 6).

While comparing, the FTIR spectra of the cellulose purified by the various processes, there is only slight shift in absorption peaks. The emergence of and disappearance of peaks were observed in the comparative FTIR spectra (Table

Table 6: Band assignment of FTIR spectrum of cellulose obtained from fifth purification method

Wavenumber (cm^{-1})	Functional group	References
3347	OH stretching	Hashim *et al.* (2021), Moharram and Mahmoud (2008), Vazquez *et al.* (2013), Hassan *et al.* (2015), Uzyol *et al.* (2017)
2897	CH stretching	Oliveira *et al.* (2015)
1645	C=O stretching	Li *et al.* (2015)
1543	CH	Irham *et al.* (2020)
1428	CH_2 bending	Hassan *et al.* (2015), Vazquez *et al.* (2013), Halib *et al.* (2012), Pandey *et al.* (2014)
1364	CH_3 deformation	Costa *et al.* (2011)
1336	OH	Vazquez *et al.* (2013), Castro *et al.* (2012), Costa *et al.* (2011)
1281	CH deformation	Popescu *et al.* (2007)
1236	C-O-C	Sepperumal *et al.* (2014)
1202	OH plane bending	Popescu *et al.* (2007), Vazquez *et al.* (2013)
1161	C-O-C	Uzyol and Sacan (2017), Casaburi *et al.* (2018), Amin *et al.* (2012), Hassan *et al.* (2015), Auta *et al.* (2017), Pandey *et al.* (2014), Costa *et al.* (2011)
1111	C-C	Dayal *et al.* (2013), Sepperumal *et al.* (2014)
1065	C-O-C	Moosavi and Yousefi (2010), Vazquez *et al.* (2013), Kuo *et al.* (2016)
897	C-O-C	Dayal *et al.* (2013), Pandey *et al.* (2014)
668	CH Rocking	Irham *et al.* (2020)
619	CH	Kondo *et al.* (2016)

Table 7: Comparative band assignment of FTIR spectra of BC obtained from five different methods

Method 1	Method 2	Method 3	Method 4	Method 5
3349 (OH)	3480 (OH)	3349 (OH)	3348 (OH)	3347 (OH)
2919 (CH)		2898(CH)	2921(CH)	2897(CH)
2852 va(CH_2)				
	2472(O-D)			
	1760(C=O)			
1651(C=O)	1653(C=O)	1647(C=O)	1650(C=O)	1645(C=O)
	1596(C=C)			
1559(CH)		1550(CH)	1548(CH)	1543(CH)
	1511(C=C)			
	1439(COOH)			
1428(CH_2)		1428(CH_2)	1427(CH_2)	1428(CH_2)
			1400(CH_2)	
1372(CH_3)	1375(CH_3)	1366(CH_3)	1375(CH_3)	1364(CH_3)
1337(OH)		1336(OH)		1336(OH)
1317(CH_2)				
1281(CH)		1281(CH)		1281(CH)
1234(C-O-C)		1236(C-O-C)		1236(C-O-C)
1204(OH)	1202(OH)	1202(OH)	1205(OH)	1202(OH)
1162(C-O-C)	1159(C-O-C)	1161(C-O-C)	1161(C-O-C)	1161(C-O-C)
1111(C-C)	1116(C-C)	1111(C-C)	1111(C-C)	1111(C-C)
1060(C-O-C)		1061(C-O-C)	1060(C-O-C)	1065(C-O-C)
1036(C-O)		1037(C-O)	1036(C-O)	
895(C-O-C)		897(C-O-C)	892(C-O-C)	897(C-O-C)
	865(CH)			
	685(CH)			
669(CH)	665(CH)	668(CH)	668(CH)	668(CH)
618(CH)	622(CH)	618(CH)	618(CH)	619(CH)

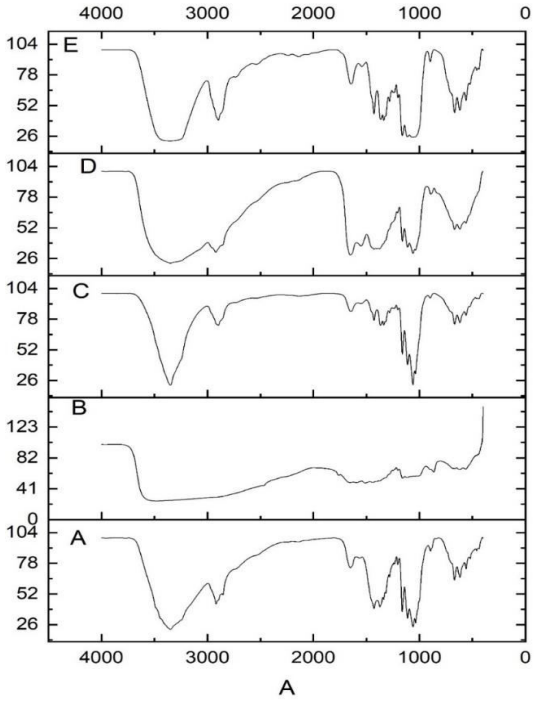

Fig. 7: Comparative FTIR spectra of BC produced by various purification processes.

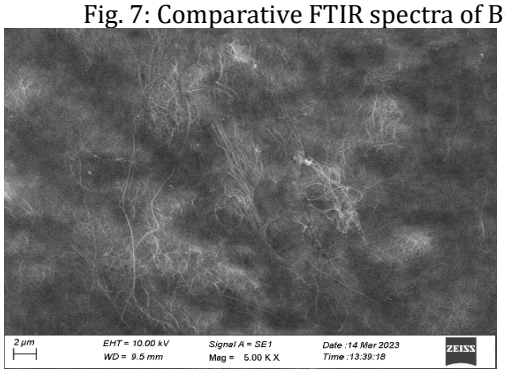

Fig. 8

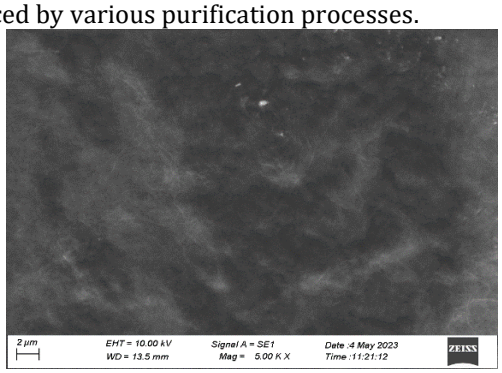

Fig. 9

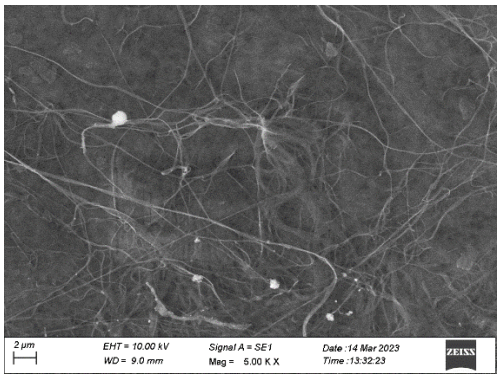

Fig. 10

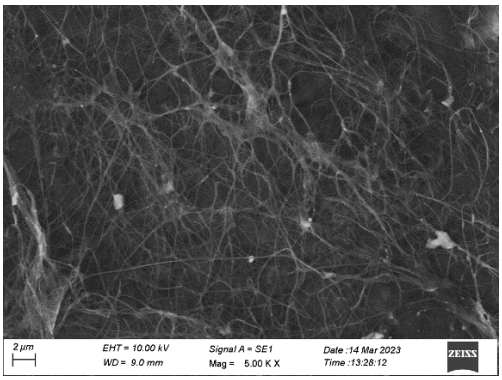

Fig. 11

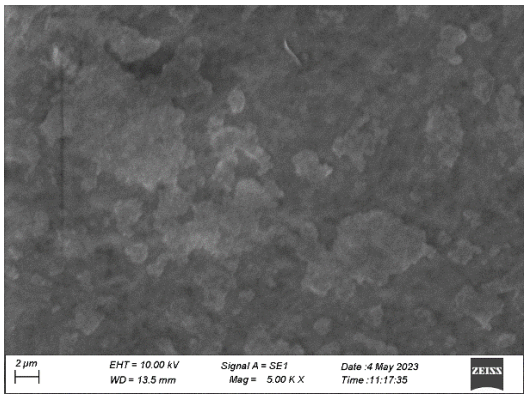

Fig. 12

7). Moreover, variations in the intensity of these absorption peaks have been evinced (Figure 7).

SEM Analysis:

SEM images of BC purified by various purification processes. Figures 8-12 displays SEM images of dried films of BC obtained by five different purification procedures. Except Figure 11, all other Figures exhibited the characteristic network structure attributed to native BC. Good loose fibrillar network of BC was observed in Figures 10 and 11 (purification processes 3 and 4). The detailed examination of these images clearly indicates the morphological differences of BC sheets obtained from various purification processes.

Conclusion

Five distinct techniques were employed to effectively purify the BC membranes. Furthermore, there is no noticeable changes in terms of the chemical properties or the amount of weight reduction. The SEM images reveals distinct morphological changes. The best result given by the fourth method.

Conflict of Interest

The authors declare no conflicts of interest.

References

Amin MCIM, Abadi AG, Ahmad N, Katas H and Jamal JA. (2012) Bacterial cellulose film coating as drug delivery system: physicochemical, thermal and drug release properties. Sains Malaysiana 41(5): 561-568.

Auta R, Adamus G, Kwiecien M, Radecka I and Hooley P. (2017) Production and characterization of bacterial cellulose before and after enzymatic hydrolysis. African J Biotechnol. 16(10): 470-482.

Cakar F, Ozer I, Aytekin AO and Şahin F. (2014) Improvement production of bacterial cellulose by semi-continuous process in molasses medium. Carbohydrate Polymers 106: 7-13.

Casaburi A, Rojo UM and Cerrutti P. (2018) Carboxymethyl cellulose with tailored degree of substitution obtained from bacterial cellulose. Food Hydrocolloids 75: 147-156.

Castro C, Zuluaga R, Alvarez C, Putaux J L, Caro G, Rojas O J, Mondragon I and Ganan P. (2012) Bacterial cellulose produced by a new acid-resistant strain of *Gluconacetobacter* genus. Carbohydrate Polymers 89(4):1033-1037.

Chen P, Cho SY and Jin HJ. (2010) Modification and applications of bacterial celluloses in polymer science. Macromolec Res. 18(4): 309-320.

Costa LMM, de Olyveira GM, Basmaji P and Filho LX. (2011) Bacterial cellulose towards functional green composites materials. J Bionanosci. 5(2):167-172.

Dayal MS, Goswami N and Sahai A. (2013) Effect of media components on cell growth and bacterial cellulose production from *Acetobacter aceti* MTCC 2623. Carbohydrate Polymers 94(1): 12-16.

Guzel M and Akpinar O. (2019) Production and characterization of bacterial cellulose from citrus peels. Waste Biomass Valorization 10: 2165-2175.

Halib N, Amin MCIM and Ahmad I. (2012) Physicochemical properties and characterization of

Nata De Coco from local food industries as a source of cellulose. Sains Malaysiana 41(2): 205-211.

Hashim NARNA, Zakaria J, Mohamad S, Mohamad SFS and Rahim MHA. (2021) Effect of different treatment methods on the purification of bacterial cellulose produced from OPF juice by *Acetobacter xylinum*. IOP Conf Ser Mater Sci Eng 1092(1): 2058.

Hassan EA, Abdelhady HM, El-Salam SSA and Abdullah SM. (2015) The characterization of bacterial cellulose produced by *Acetobacter xylinum* and *Komgataeibacter saccharovorans* under optimized fermentation conditions. British Microbiol Res J. 9(3): 1-13.

Huang Y, Zhu C and Yang J. (2014) Recent advances in bacterial cellulose. Cellulose 21: 1-30.

Irham WH, Tamrin, Marpaung L and Marpongahtun (2020) Characterization of bacterial cellulose from coconut water supplemented Curcuma Longa Linn and Ziziphus Mauritiana extract. AIP Conf Proc. https://doi.org/10.1063/5.0023953

Kamal ASM, Misnon MI and Fadil F. (2020) The effect of sodium hydroxide concentration on yield and properties of bacterial cellulose membranes. IOP Conf Ser Mater Sci Eng. 732(1): 2064.

Kondo T, Rytczak P and Bielecki S. (2016) Bacterial nanocellulose characterization. In: Bacterial Nanocellulose, (eds.) Miguel G., Fernando D., and Stanislaw B., Elsevier, pp. 59-71.

Kuo CH, Chen JH, Liou BK and Lee CK. (2016) Utilization of acetate buffer to improve bacterial cellulose production by *Gluconacetobacter xylinus*. Food Hydrocolloids 53: 98-103.

Li Z, Wang L, Hua J, Jia S and Zhang J. (2015) Production of nano bacterial cellulose from waste water of candied jujube-processing industry using *Acetobacter xylinum*. Carbohydrate Polymer 120: 115-119.

Moharram MA and Mahmoud OM. (2008) FTIR spectroscopic study of the effect of microwave heating on the transformation of cellulose I into cellulose II during mercerization. J App Poly Sci. 107(1): 30-36.

Moniri M, Moghaddam AB, Azizi S, Rahim RA, Ariff AB, Saad WZ, Navaderi M and Mohamad R. (2017) Production and status of bacterial cellulose in biomedical engineering. Nanomaterials 7(9): 257.

Moosavi-Nasab M and Yousefi AR. (2010) Investigation of physicochemical properties of the bacterial cellulose produced by *Gluconacetobacter xylinus* from date syrup. World Acad Sci Engineer Technol. 44: 1258-1263.

Oliveira RL, Vieira JG, Barud HS, Assuncao RMN, Filho GR, Ribeiro SJ and Messadeqq Y. (2015) Synthesis and characterization of methylcellulose produced from bacterial cellulose under heterogeneous condition. J Braz Chem Soc. 26: 1861-1870.

Pandey M, Abeer MM and Amin MCI. (2014) Dissolution study of bacterial cellulose (nata de coco) from local food industry: Solubility behavior and structural changes. Int J Pharm Pharm Sci. 6(6): 89-93.

Popescu CM, Popescu MC, Singurel G, Vasile C, Argyropoulos DS and Willfor S. (2007) Spectral characterization of eucalyptus wood. Appl Apectroscopy 61(11): 1168-1177.

Saibuatong OA and Phisalaphong M. (2010) Novo aloe vera–bacterial cellulose composite film from biosynthesis. Carbohydrate Polymers 79(2): 455-460.

Sepperumal U, Selvanayagam S and Markandan M. (2014) Characterisation of cellulose produced by *Pseudomonas sp*. and *Actinomycetes sp*. European J Zool Res. 3(4):13-18.

Shezad O, Khan S, Khan T and Park JK. (2010) Physicochemical and mechanical characterization of bacterial cellulose produced with an excellent productivity in static conditions using a simple fed-batch cultivation strategy. Carbohydrate Polymers 82(1): 173-180.

Tsouko E, Kourmentza C, Ladakis D, Kopsahelis N, Mandala I, Papanikolaou S, Paloukis F, Alves V and Koutinas A. (2015) Bacterial cellulose production from industrial waste and by-product streams. Int J Mol Sci. 16(7): 14832-14849.

Umamaheswari S and Naveena K. (2017) FTIR spectral and microarchitectural analysis of cellulose produced by *Lactococcus lactis* under agitated condition. J Pure Appl Microbiol 11(4): 1965-1971.

Uzyol HK and Sacan MT. (2017) Bacterial cellulose production by *Komagataeibacter hansenii* using algae-based glucose. Environ Sci Pollut Res. 24: 11154-11162.

Vazquez A, Foresti ML, Cerrutti P and Galvagno M. (2013) Bacterial cellulose from simple and low-cost production media by *Gluconacetobacter xylinus*. J Poly Env. 21: 545-554.